Study on Statistical Prediction and Design Method for Indoor Thermal Environment

You Zhou[1], Kyosuke Hiyama*[2], Shinsuke Kato[3] and Weirong Zhang[4]

[1] Graduate Student, School of Engineering, the University of Tokyo, Japan
[2] Associate Professor, Faculty of Engineering, Yamaguchi University, Japan
[3] Professor, Institute of Industrial Science, the University of Tokyo, Japan
[4] Project Researcher, Institute of Industrial Science, the University of Tokyo, Japan

Abstract

The indoor thermal environment is affected by many heat factors such as occupants' activities and outdoor climate changes. Because each of them varies asynchronously, the heat factors' variation shows a nonsingle degree of freedom overall. Moreover, the heat factors' impact on space is not uniform. Therefore, there always exist spatial distributions and temporal variations.

In practice, the number of degrees of freedom of an air-conditioning system is usually limited and less than that of the object zone. The control performance of an air-conditioning system designed under a perfect mixing method cannot be satisfactory because the spatial distribution is neglected. For energy conservation and thermal comfort improvement, it is necessary to propose an air-conditioning system design method which can positively use the spatial distribution and temporal variation of the indoor thermal environment.

In this study, methods for indoor temperature fluctuation analysis and optimization of air-conditioner sensor location are proposed. To represent the temperature field structure, an index called CRI is integrated. With this method, the spatial distribution and temporal variation can be calculated immediately and analyzed statistically; furthermore, the indoor temperature and outdoor climate's correlation can be concisely visualized. A case study is conducted to verify the validity of this method.

Keywords: spatial distribution; temporal variation; indoor temperature fluctuation analysis; indoor temperature control; optimization of air-conditioner sensor location

1. Introduction

To create an indoor thermal environment that can realize energy conservation and improve thermal comfort, an air-conditioning system that can positively utilize the spatial distribution and temporal variation of the indoor temperature is of importance.

Many heat factors affect the indoor thermal environment. Some vary periodically depending on outdoor climate changes, whereas others may vary depending on the occupants' behaviors. The variation of all heat factors is not synchronous, and each factor has its own variation schedule. The overall result of the heat factors' variation shows a nonsingle degree of freedom. Moreover, different indoor locations show different sensitivity toward changes in heat loads.

When handling such a thermal environment, theoretically, the ideal strategy is to use an air-conditioning system with equivalent degrees of freedom. However, in practice, owing to limitations such as cost control, the number of degrees of freedom of the air-conditioning system is usually less than that of the object zone.

Conventionally, a perfect mixing method is commonly used[1]. To ensure that the indoor temperature variation is as small as possible, heat input to the zone should be dispersed promptly. As an evaluation measure, ASHRAE proposed the Air Diffuse Performance Index (ADPI)[2], a criterion that describes the indoor efficient draft temperature[3], to aid the design of air inlet conditions that can create a space with a small temperature distribution. The spatial distribution is ignored, so the sensor positions are considered arbitrary, and they are only designated to monitor the temporal variation alone. Perfect mixing conditions imply that entropy is maximized, in which case control of the spatial distribution becomes unnecessary. As a result, the air-conditioners' sensors only need to monitor the temporal variation.

Clearly, this method fails to exploit the spatial temperature distribution. As the maximization of entropy also leads to an increase in the energy consumption, some energy is wasted. Furthermore, by using this method, the entire thermal environment becomes uniform, making it very difficult to meet the needs of each individual occupant. For example, it is unsuitable for designing task-ambient air-conditioning,

*Contact Author: Kyosuke Hiyama, Associate Professor, Yamaguchi University,
2-16-1 Tokiwadai Ube-shi Yamaguchi, 755-8611, Japan
Tel: +81-836-85-9711
E-mail: hiyama@yamaguchi-u.ac.jp
(Received April 12, 2013 ; accepted November 11, 2013)

which is considered beneficial for both saving energy and enhancing comfort. Therefore, to create an indoor thermal environment that can satisfy both energy-saving and individual requirements, it is necessary to consider both the spatial distribution and temporal variation of the indoor thermal environment.

In recent years, design based on 3D CFD analysis has attracted much attention. Steady CFD analysis using constant boundary conditions is widely used to support design. However, this method focuses on the spatial distribution alone, and it cannot provide results about the temporal variation within a period.

Another proposal is unsteady CFD analysis, which considers transient boundary conditions; this approach can be used to express the temperature sequences in time series, for instance, under automated control of air-conditioners. However, unsteady CFD analysis requires considerable time and computational resources. Thus, this method, although theoretically feasible, is currently unsuitable for practical use.

To overcome these problems, the authors propose a new method that is characterized by the use of sensitivity analysis of heat sources to a target space. Here, the heat sources include heat loads as well as heat release from the air-conditioning system.

As mentioned before, controlling systems are usually confined to a lesser number of degrees of freedom than the target zone. The air-conditioning motion is dependent on the signal from the sensor, and most sensors only monitor the thermal environment that it is assigned. Thus, the controlling system usually has fewer sensors than the resolution of the space it controls. In this situation, the best sensor location is the one where the sensitivity between the air-conditioning motion and the temporal variation of the indoor thermal environment is minimized. In other words, it is important to place the sensor at a location that can improve its robustness to the thermal environment against variation of heat loads.

The contribution ratio of indoor climate (CRI) for sensitivity analysis is employed in this study. The CRI[4] proposed by Kato *et al.* treats the velocity field as fixable for a small variation range of the inlet air temperature (Sempey *et al.*, 2009)[5] and the temperature field as an approximately linear system. CRI provides information about the temperature field's spatial structure and the analyses using CRI require much less calculation time and computational resources than normal unsteady CFD analysis.

To ensure that the target space of an air-conditioning system shows the maximum possible robustness against variation in heat loads, the air-conditioner's sensor should be well representative of the target space. As mentioned above, CRI can be used to determine any location's spatial sensitivity and characteristics of temperature fluctuation, and therefore, an air-conditioner's sensor location can be quantitatively discussed by using CRI.

In this study, methods for indoor temperature fluctuation analysis and optimization of the air-conditioner's sensor location are proposed. CRI can be used to calculate the spatial distribution and temporal variation in real time, and the correlation between the indoor temperature and the outdoor climate' can be concisely visualized. To verify the validity of this method, a case study is conducted by evaluating and comparing an air-conditioner and its various sensor locations.

2. Related Work

Harayama *et al.* proposed a local thermal environment control technology based on reversed CFD analysis and a position detection technique with the aim of temperature control at any location in a room[6][7]. His proposed reversed CFD analysis is in contrast to normally known CFD analysis, with boundary conditions such as the air flow and temperature distribution as its output. Then, Harayama *et al.* developed a new simulator called Ambican to evaluate the air-conditioning performance, effect of energy conservation, and comfort of target zone[8][9].

Moreover, as with the concept of reversed CFD analysis, Honda *et al.* presented an HVAC control method based on fuzzy models in large spaces that is characterized by the prediction of temperature and air flow distribution independently of the sensor location[10]. Based on simplified fuzzy theory, CFD analysis is conducted using the air-conditioning and operation conditions as parameters. Then, the steepest descent method is applied to calculate the membership functions that can minimize the prediction errors.

Harayama *et al.* mentioned two reversed CFD analysis methods[7]. One was proposed by Momose *et al.* (2004)[11]. The sensitivity of the thermal boundary is calculated by using a reversed simulation based on adjoint numerical analysis; then, by applying the functional derivative in the gradient-based method, the improvement in the heat transfer characteristics can be analyzed. The other is the CRI proposed by Kato *et al.* (1998)[4], which treats the thermal environment as a linear system, to easily analyze the influence of each heat factor and thermal environment in a short period.

By using CRI, Hiyama and Zhang *et al.* presented an energy simulation method by coupling a network model and a CFD simulation. Hiyama developed a method that can calculate any location's temperature change quickly using the transient heat response on a static flow field and can also calculate the energy consumption of long-term unsteady conditions combined with a dynamic heat load calculation method that can analyze the heat transport inside walls[12][13]. Zhang introduced a new CRI index when the target zone is under natural ventilation and proposed a new energy simulation method that covers air-conditioning and natural ventilation[14][15].

In these previous researches, the sensor is based on the occupant's locations and not the point that can best represent the target zone. This may lead to inefficient air-conditioning in the target zone. Furthermore, the proposed control technology focuses on the operation rather than the design phase. As the initial design of a building determines its future energy consumption

performance, a method that can aid the design process is of great importance. The awareness of how long and where the desired thermal condition can be maintained will greatly help designers and mechanics.

3. Method

3.1 Room Temperature Fluctuation Analysis

3.1.1 Relation between heat sources and temperature

The structure and formation of a temperature field can be indicated by using CRI in the form of each heat's contribution ratio, so the distribution properties can be analyzed clearly. As for the definition of CRI, heat sources need to be specially considered. Because convective heat transfer from heat sources is what directly and eventually affects the indoor air temperature, only convective heat transfer from heat sources is taken into consideration. Radiant heat transfer, being simply a process of heat transfer, is ignored. Therefore, all the heat factors involved in convective heat transfer are treated as heat sources.

In this light, although insulated walls do not release heat themselves, they are heated or cooled by radiation heat transfer from other heat sources and are then involved in convective heat transfer. Therefore, they are defined as heat sources as well.

There are several types of CRIs (Kato *et al.* 1998)[4]; however, in this study, only CRI 1 (hereafter referred to as simply "CRI") is applied. It is calculated by dividing the actual temperature rise or drop by the homogenous temperature rise or drop under perfect mixing assumption, and it is dimensionless. Eqs. (1) and (2) below show how CRI is calculated.

$$\mathrm{CRI}_i(X) = \frac{\mathrm{d}\theta_i(X)}{\theta_0} \quad (1) \qquad \theta_0 = \frac{q_i}{c_P \cdot \rho \cdot Q} \quad (2)$$

$\mathrm{CRI}_i(X)$: CRI at point X corresponding to heat source i (-)
$\mathrm{d}\theta_i(X)$: temperature rise or drop at point X (°C) when heat q_i (W) is released from heat source i (convective heat transfer)
θ_0: temperature rise or drop under perfect mixing conditions when heat q_i (W) is released from heat source i (convective heat transfer) (°C)
q_i: heat released from heat source i (W)
Q: supply air volume (m^3/h)
$C_p \cdot \rho$: volumetric specific heat of air ($Wh/(°C \cdot m^3)$)

When CRI equals 1, it means that for the heat source concerned, the location has the same sensitivity as under perfect mixing conditions. Similarly, when there is only one air inlet, CRI of the heat from air inlet will equal 1 anywhere in the space, because the air inlet's influence over the entire space is uniform.

The indoor temperature can be shown by Eq. (3). Eq. (3) shows that there are n degrees of freedom at an arbitrary point X in the space. However, some heat sources have a strong correlation with others (i.e., heat transfer through exterior walls varies with the outdoor climate). Therefore, grouping heat sources according to their schedules can reduce the system's degrees of freedom and simplify the analysis.

$$\theta(X) = \theta_n + \sum_{i=1}^{n} \Delta\theta_i(X) = \theta_n + \sum_{i=1}^{n} (\mathrm{CRI}_i(X) \cdot q_i) \quad (3)$$

θ_n: neutral temperature (°C), air temperature when there is no heat source.

3.1.2 Relation between sensor and any other point temperature at an arbitrary point

In an air-conditioned room, the air-conditioner keeps modifying variables, such as the supply air temperature, to ensure that the temperature detected by the sensor is always within the desired levels. The relation between the sensor and the temperature at an arbitrary point can be described using CRI.

When a minor change occurs in the heat source, this leads to temperature fluctuation at an arbitrary point X including the sensor position S. The temperature fluctuation can be calculated by Eqs. (4) and (5).

$$\mathrm{d}\theta_i(X) = \mathrm{CRI}_i(X) \cdot \mathrm{d}q_i \quad (4)$$
$$\mathrm{d}\theta_i(S) = \mathrm{CRI}_i(S) \cdot \mathrm{d}q_i \quad (5)$$

$\mathrm{d}\theta_i(S)$: temperature rise or drop at sensor position S when there is a minor change $\mathrm{d}q_i$ in heat source I (convective heat transfer) (°C)
$\mathrm{d}q_i$: heat change in heat source i (W)

When the air-conditioning is of a constant air volume (CAV) type, to cancel out the temperature fluctuation detected by the sensor, the air-conditioner will modify the supply air temperature. As explained in 3.1.1, in the case of a single air-conditioner, the air inlet's CRI is independent of the location and equals 1 uniformly within the space. Consequently, the supply air's temperature change is identical to the sensor's temperature fluctuation. This is given by Eq. (6).

$$\mathrm{d}\theta_{\mathrm{ac}} = -\mathrm{d}\theta_i(S) = -\mathrm{CRI}_i(S) \cdot \mathrm{d}q_i \quad (6)$$

$\mathrm{d}\theta_{\mathrm{ac}}$: temperature change of supply air (°C)

Consequently, the supply air's temperature change will affect the entire indoor space homogenously. As a result, given that the supply air temperature is modified instantly, the temperature fluctuation at any point X can be calculated as given by Eq. (7).

$$\mathrm{d}\theta_i(X) = \mathrm{CRI}_i(X) \cdot \mathrm{d}q_i + \mathrm{d}\theta_{\mathrm{ac}} = \big(\mathrm{CRI}_i(X) - \mathrm{CRI}_i(S)\big) \cdot \mathrm{d}q_i \quad (7)$$

3.2 Optimization of Air-Conditioner Sensor Location

To maintain the room temperature within the desired levels to the greatest extent possible, the ideal strategy is to set as many sensors as the resolution of the target space. However, in real projects, only a limited number of sensors can be placed at limited locations. Thus, a practical solution is to specify the installment location of which the temperature detected by the sensor can best represent the entire space.

To evaluate the representativeness of a location, its total integral of temperature differences with all the

other spaces, both spatial and temporal, can be used as a benchmark (Eq. 8). If the sensor location has the best representativeness compared to others, this value $D(X)$ will become the smallest.

$$D(X) = \int_T \int_V |\Delta T_{si}(X)| \, dV dt \quad (8)$$

$D(X)$: total integral of temperature differences with all the other spaces when sensor is set at point X (°C)
$\Delta T_{si}(X)$: at time step i, integral of temperature differences with point s when sensor is set at point X (°C)
V: volume of the entire space
T: calculation period

Moreover, the scope of the sensor is of importance. Actually, the target space of air-conditioning may sometimes be just a part of the room rather than the entire space. When a proportion of the target space (i.e., occupancy zone) reaches the desired value preferentially, the temperature deviation of other spaces (i.e., space around ceiling) from the desired levels can be tolerated. This preference difference, if utilized positively, can reduce energy consumption.

To combine this preference difference toward the space, the weighting factor K is introduced (Eq. 9). Every temperature difference with a certain point will be multiplied by a weighting factor that is determined by where this point is located. The more important the place where the point is located, the larger weighting factor K the integral will be multiplied with. In this manner, the sensor location can be optimized by evaluating the newly defined value $D'(X)$: the total spatial and temporal integral of the temperature difference combined with the weighting factors.

Furthermore, by modifying each point's weighting factor, various demands on the indoor thermal environment can be satisfied.

$$D'(X) = \int_T \int_V K_s |\Delta T_{si}(X)| \, dV dt \quad (9)$$

$D'(X)$: total integral of temperature differences with all the other spaces when sensor is set at point X, combined with point X's weighting factor (°C)

In Table 1., each point's temperature is shown horizontally and its temporal variation, vertically. The spatial and temporal integral calculation can be discretized into the sum of temperature difference of scattered examination point grid nodes at each time step. The equation is given by Eq. (10).

Table 1. Time Series of Each Point's Room Temperature

	Point A	Point B	Point C	…	Point N
K	K_A	K_B	K_C	…	K_N
t_1	T_{A1}	T_{B1}	T_{C1}	…	T_{N1}
t_2	T_{A2}	T_{B2}	T_{C2}	…	T_{N2}
…	…	…	…	…	…
t_m	T_{Am}	T_{Bm}	T_{Cm}	…	T_{Nm}

$$\begin{aligned} S(X) &= \sum_{t=1}^{m} \sum_{i=1}^{N} K_s \cdot \Delta T_{si}(X) \\ &= K_A|T_{S1} - T_{A1}| + K_B|T_{S1} - T_{B1}| + \cdots + K_N|T_{S1} - T_{N1}| \\ &+ K_A|T_{S2} - T_{A2}| + K_B|T_{S2} - T_{B2}| + \cdots + K_N|T_{S2} - T_{N2}| + \cdots \\ &+ K_A|T_{Sm} - T_{Am}| + K_B|T_{Sm} - T_{Bm}| + \cdots + K_N|T_{Sm} - T_{Nm}| \end{aligned} \quad (10)$$

S (X): total sum of temperature differences with all the other spaces when sensor is set at point X (°C)
points A, B, C, ..., N: examination point grid nodes.
K_A, K_B, K_C, ..., K_N: every node's weighting factor.
t_1, t_2, t_3, ..., t_m: time series.

When the sensor is located at the place that has the smallest discretized sum of temperature difference, the examination point grid's temperature deviation from the desired value will become the smallest. Moreover, by modifying the weighting factors, the preferred zone can reach the desired temperature preferentially.

3.3 Algorithm of the Proposed Design Method

The algorithm of the proposed design method is shown in Fig.1. The procedure is briefly listed below, and will be explained in the following case study.

Step 1. Provision and modeling
Step 2. Periodic energy simulation
Step 3. Calculation of CRI
Step 4. Calculation of temperature fluctuation
Step 5. Optimization of sensor arrangement

This method is characterized methodologically by the full consideration of the spatial distribution and temporal variation, and technically by the combination of periodic energy simulation, steady CFD simulation and Excel calculations. Except for the time required for modeling and modification during the CFD process, it is nearly as fast as the network energy simulation and as accurate as the CFD calculation. Therefore, it can serve as a promising design method for both designers and engineers.

4. Case Study

A case study is conducted for the explanation and verification of the authors' proposed design method. The target is the optimization of a single-sensor arrangement in the living room of a detached house.

4.1 Provision and Modeling

In this study, the Standard house model proposed by IBEC is chosen[16] (hereafter referred to as IBEC Standard house), and the living room at the first floor is the object space to be discussed. Some furniture such as sofas and desks are assumed in the living room and the space around them is defined as the occupancy zone. Six cases are set according to the arrangement of the air-conditioner and its sensor. Cases with the air-conditioner on the south and the east exterior wall are respectively defined as Patterns 1 and 2. Furthermore, each pattern is divided into three cases: wireless sensor on the desk (Cases 1 and 4), body thermo at air inlet (Cases 2 and 5), and hybrid type (Cases 3 and 6) that combines wireless sensor and body thermo in a 1:1 ratio (system output).

4.2 Periodic Energy Simulation

Periodic energy simulation is carried out for the entire building model, and the time series of the heat

gain from every heat source is obtained.

The calculation conditions are shown in Table 2. Briefly, heating in the winter is considered, and the heating loads comprise lighting and heat transfer through walls and windows. The lights are turned on from 0600 to 2000 and from 1700 to 2300 every day.

The light on the east part of the ceiling, with 60 W heat release, is called light 1, and the light immediately above the desk, with 90 W heat release, is called light 2. Thus, the total lighting load is 150 W.

The calculation is conducted at time steps of every hour. At every time step, the heat transfer from the indoor airflow is assumed to be completed. With regard to air-conditioning, it is assumed that the air inlet temperature is modified to be identical to the desired value at every time step instantly.

TRNSYS ver.17 is used as the energy simulation tool. To simplify the calculation, transmission of solar irradiance through windows and air change between rooms are not considered.

4.3 Calculation of CRI [Note 1)]

In 59 days of periodic energy simulation, the review period is 30 days, from Jan 16 to Feb 14 (15th day to 46th day). Here, heat sources' CRIs are calculated[14)15)]. First, the flow field is calculated with all heat sources in action. This field is called the original flow field. The heat flux of each boundary is set according to the results in the periodic energy simulation. Here, the periodic mean values of the heat gains from heat sources are taken as the representative values and are applied to the calculation. Airflow is injected from a 0.12 m^2 inlet at 2 m/s and in a 60° downward direction, and the same amount of air is drawn out by a 0.12 m^2 outlet at the top of the air-conditioner. The air-conditioning is assumed to be of a CAV type. The initial supply air temperature is calculated manually under constant heat transfer simulation conditions to meet the condition that the outlet air temperature can reach 22.0°C. A commercial code, Star-CCM+, is applied and detailed conditions are shown in Table 3.

Second, the flow field is recalculated with the flow field fixed and the heat sources turned down. The recalculated flow field has the same flow field as the original flow field but a homogenous identical temperature within the entire room. Then upon the recalculated flow field, heat source is activated one by one, and the temperature rise or drop for every point is calculated.

Table 2. Calculation Conditions for Periodic Energy Simulation

Objective: IBEC Standard house (entire building)
Air-conditioning: (all day, sensible heat only) Heating: 22.0°C, January to February (59 days)
Climate conditions: Extended AMeDAS (2010) Tokyo
Walls and windows: Heat transfer coefficient (W/m^2·K) Window surface: 5.800, Ceiling: 1.629, Roof: 1.065, Floor: 0.709, Door: (exterior) 1.671; (interior) 2.591, Wall: (exterior) 1.372, (interior) 3.583, Heating storage capacity is equivalent to that of ordinary wooden houses in Japan.
Interior heat loads: Lighting: 150 W (Convective part 40%, radiative part 60%)

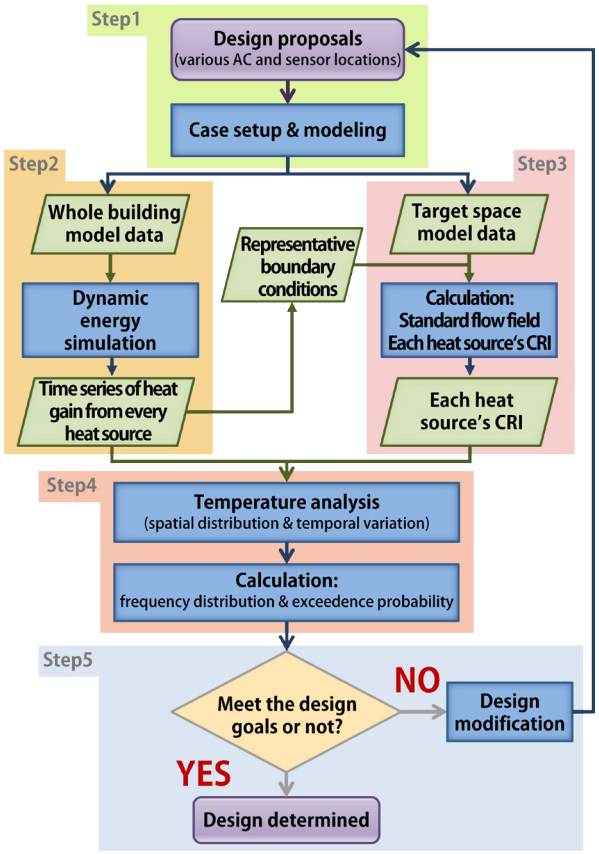

Fig.1. Procedures for Indoor Temperature Fluctuation Analysis and Optimization of Air-Conditioner Sensor Location Proposed in this Study

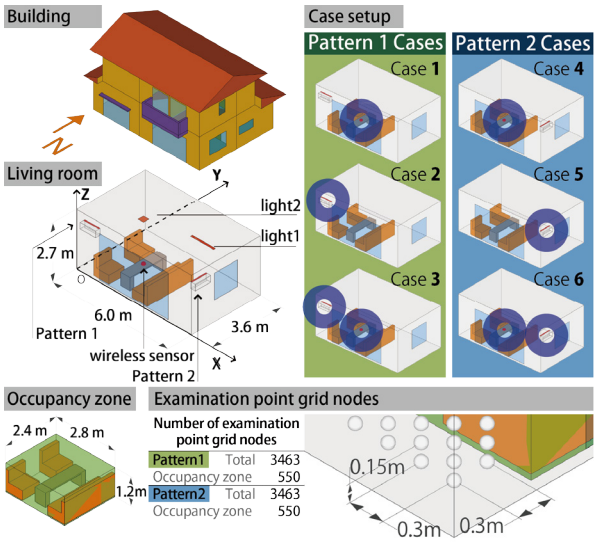

Fig.2. Analysis Model, Cases and Examination Point Grid

Table 3. Calculation Conditions for Original Flow Field

Objective: Living room at 1st floor of IBEC Standard house
Turbulence model: Standard k-ε model
Difference schemes: Advection term: two-order upwind difference scheme Diffusive term: two-order center difference scheme
Grid resolution: Pattern 1: ~210,065, Pattern 2: ~206,632
Space measurements: Living room: 6 m × 3.6 m × 2.7 m
Boundaries: Representative values of convective heat gain from interior wall obtained from energy simulation (1700 on 41st day)

Finally, the CRI for each heat source can be calculated using Eqs. (1) and (2)[14)15)].

4.4 Calculation of Temperature Fluctuation

By applying Eqs. (3) with the heat gains' time series and the CRIs of heat sources, the temperature fluctuation in the living room can be calculated and analyzed.

4.5 Optimization of Sensor Location

First, the living room space is filled with examination point grid nodes for every 0.3 m × 0.3 m × 0.15 m, for a total of 3463 nodes with 550 in the occupancy zone (Fig.2.). All the nodes are considered as candidates for the best sensor location.

Second, the weighting factors are set. Here, the authors prioritize the occupancy zone over the other spaces in the living room. The weighting factors can be added by two methods. In the first method, according to the ratio of the number of examination points in the occupancy zone to that in the other spaces, the weighting factor for the occupancy zone and the other spaces is assumed to be 5 and 1, respectively. In other words, the occupancy zone carries the same importance as the other spaces despite the difference in grid number. The second method is used to verify the validity of the weighting factors, and therefore, all the examination points are considered to have the same weighting factor of 1.

Third, sensors are placed at each node sequentially, and the difference between the sensors' and the other points' temperature throughout the entire review period is added up according to Eq. (8). Then, the points of minimum sum are selected as the optimization group and the points of maximum sum, as the reference group.

5. Results

5.1 Results of Original Flow Field

The review period is from Jan 16 to Feb 14 (15th day to 46th day), for a total of 30 days. For Patterns 1 and 2, where the air-conditioner is respectively on the south and the east wall, the original flow field's horizontal temperature distribution and east window's CRI distribution are shown in Fig.3. The average temperature of Pattern 1 is 19.9°C and that of Pattern 2 is 20.1°C. Together with the standard deviation of the total room temperature shown in Table 2., it can be concluded that the temperature distribution of Pattern 1 is more uneven than that of Pattern 2.

Because there is only one air-conditioner, the CRI for the air-conditioner as a heat source is uniform at any place in the room. Therefore, the formation of a temperature field can be understood by analyzing the distribution of the influence of other heat sources.

Here, the east window's CRI distribution is taken as an example, in Pattern 1 the east window's CRI drops greatly from the east window area to the interior space. Around the east window, cold heat has a greater influence than warm heat from the air-conditioner on the south wall. In the interior space, the cold heat's influence decreases considerably and that of warm heat from the air-conditioner increases. Thus, Pattern 1's temperature distribution becomes quite uneven. In Pattern 2, except for the east window area, the CRI distribution is approximately uniform. Cold heat from the east window and warm heat from the air-conditioner are well mixed first, following which they are carried into the inner space and dispersed.

5.2 Results of Control Performance

First, the performance in the occupancy zone is examined. The average temperature fluctuation of the occupancy zone is shown in Fig.4. Although both Patterns 1 and 2 show daily periodicity as a common feature, Pattern 2 more closely approximates the desired temperature of 22.0°C than Pattern 1 on the whole. In addition, when the air-conditioner is installed at the same location, in terms of the average temperature and stability, it can be observed that a wireless sensor on the desk is better than the hybrid type, which in turn is better than body thermo.

For the entire room, Fig.5. shows the cumulative frequency distribution and exceedance probability of the examination point grid. Compared with the cases of Pattern 1, all the cases of Pattern 2 show a slender and concentrated distribution with a larger peak value at 22.0°C. When comparing cases according to the sensor location, the hybrid type exhibits the most concentrated frequency distribution at 22.0°C, which is a characteristic common to both Patterns 1 and 2.

5.3 The Correlation between Indoor Temperature and Heating Load Fluctuations

Fig.6. shows the correlation between the temperature fluctuation of the examination point grid and the heating loads in longitudinal sections through the wireless sensor on the desk. In the color scale of Fig.6., red means a perfect positive linear correlation, which can be interpreted here as the temperature of this part increasing with the heating loads. In contrast, blue means a perfect negative linear correlation.

Because ~92.5% of the heating load is a penetrating heating load due to the outdoor thermal environment, the heating loads can be considered synchronized with the variation in the outdoor thermal environment. In this light, assuming that all the heat sources take effect simultaneously, the synthesized CRI's distribution is as shown in Fig.7. The correlation reversion phenomena in Fig.6. can be explained by Fig.7. In case 1, the synthesized CRI at the sensor location is ~1.25. In case 2, it is ~1.00. The synthesized CRI's contour in Fig.7. crossing the sensor becomes the boundary of the correlation reversion shown in Fig.6.

The room space is approximately divided into two parts by the CRI contour based on the sensor location: the exterior part relatively closer to the outdoor environment, and the interior part relatively closer to the sensor and more dominated by the air-conditioner. In the exterior part, the room temperature is positively correlated with the absolute value of heat loss through exterior walls and windows, and vice versa.

Eq. 7 explains this mathematically. When $CRI_i(X)$ - $CRI_i(S)$ is positive or negative, $d\theta_i(X)$ monotonically increases or decreases with an increase in dq_i. Thus, within a space where $CRI_i(X)$ - $CRI_i(S)$ is positive,

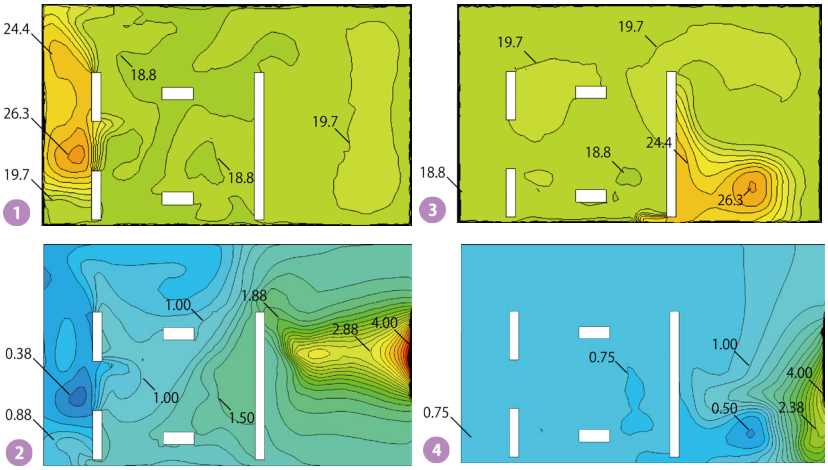

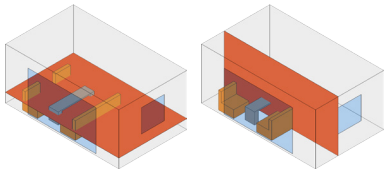

horizontal section z = 0.5 m　　vertical section y = 1.2 m

Fig.1. CRI Calculation Results
Pattern 1, Results of original flow field (standard condition, horizontal section)
1. Temperature distribution
2. East window's CRI distribution
Pattern 2, Results of original flow field (standard condition, horizontal section)
3. Temperature distribution
4. East window's CRI distribution

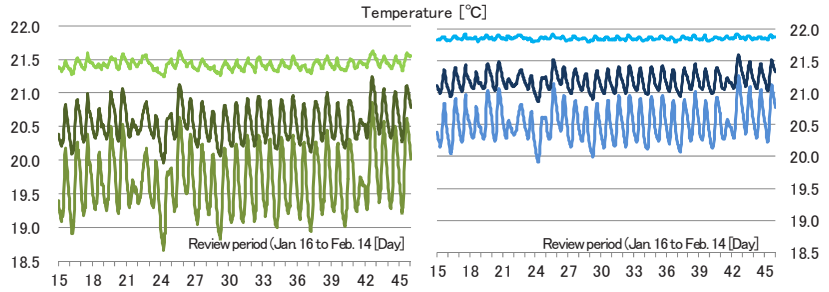

Fig.4. Average Temperature Fluctuation of Occupancy Zone. (Pattern 1: left, Pattern 2: right)

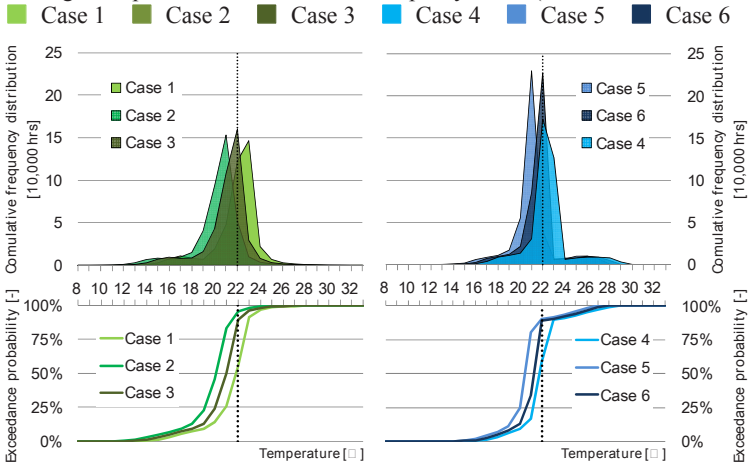

Fig.5 Cumulative Frequency Distribution and Exceedance Probability of Room Temperature (Pattern 1: left, Pattern 2: right)

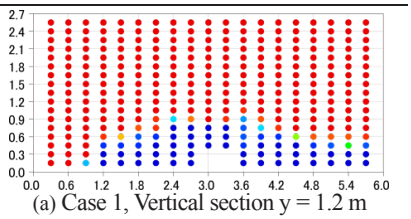

(a) Case 1, Vertical section y = 1.2 m

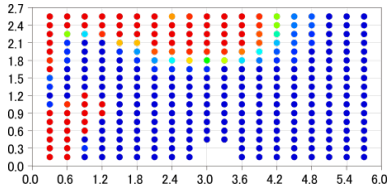

(b) Case 2, Vertical section y = 1.2 m

Fig.6. Spatial Distribution of Correlation Between Room Temperature and Heating Load

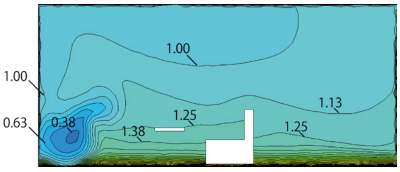

Fig.7. Synthesized CRI Distribution of Pattern 1 (Vertical Section y = 1.2 m)

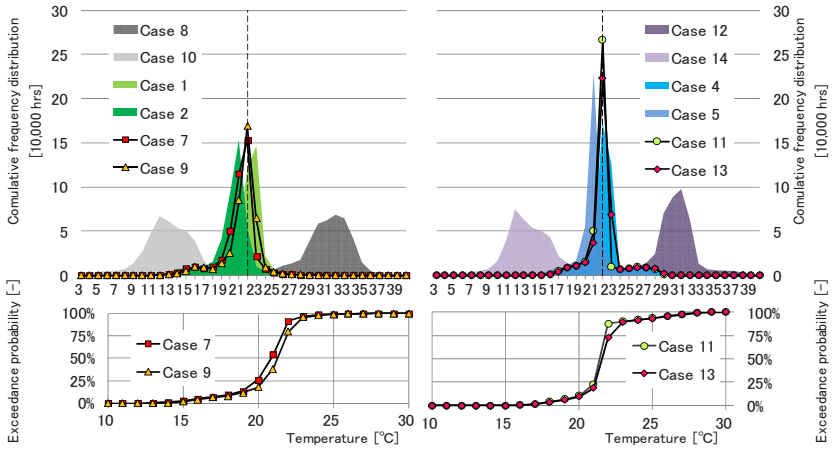

Fig.8. Frequency Distribution and Exceedance Probability of Occupancy Zone Temperature (optimization group, reference group, and previous Cases 1, 2, 4, and 5)

Table 4. Standard Deviation of Total Room Temperature

Case 1	2.013	Case 8	2.666
Case 2	2.016	Case 9	2.007
Case 3	2.006	Case 10	2.616
Case 4	1.430	Case 11	1.428
Case 5	1.438	Case 12	1.853
Case 6	1.428	Case 13	1.429
Case 7	2.006	Case 14	2.191

Table 5. Standard Deviation of Occupancy Zone Temperature

Case 1	1.944	Case 8	2.468
Case 2	1.991	Case 9	1.950
Case 3	1.958	Case 10	2.727
Case 4	1.818	Case 11	1.820
Case 5	1.838	Case 12	2.118
Case 6	1.824	Case 13	1.819
Case 7	1.960	Case 14	2.531

Table 6. Locations of Optimization Group and Reference Group

Weighting factor K	Case No.	Ranking of S (total difference in temperature)	Location [m] X	Y	Z
Pattern 1 (air-conditioner on south wall)					
$K = 1$	7	Min.	4.5	2.1	1.35
	8	Max.	5.1	0.3	0.15
$K = 5$	9	Min.	1.5	1.5	1.20
	／	Max.※	5.1	0.3	0.15
	10	2nd Max.	0.9	0.3	1.65
Pattern 2 (air-conditioner on east wall)					
$K = 1$	11	Min.	1.5	2.4	2.25
	12	Max.	4.2	2.1	0.15
$K = 5$	13	Min.	2.4	1.2	1.05
	14	Max.	5.7	0.9	1.65

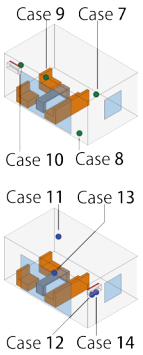

Note: For $K = 5$, take the second-largest S as Case 10 because the max. point turns out to be the same when the weighting factor is 1 and 5.

the space temperature is positively correlated with the change in the exterior heat load, and vice versa.

In this manner, by visualizing the contribution ratio of each heat source in the form of CRI, the influence of the sensor location can be analyzed along with the characteristics of the room temperature fluctuation.

5.4 Optimization of Sensor Arrangement

Sensor locations of the optimization group and the reference group are shown in Table 6. In Fig.8., the frequency distribution and exceedance probability of the examination point grid in the occupancy zone are shown when the sensor is set according to Table 6., together with the results of Cases 1, 2, 4, and 5 that also use a single sensor. Compared to Cases 1, 2, 4, and 5, the optimization group (Cases 7, 9, 11, and 13) show a more concentrated frequency distribution and a much higher frequency at 22.0°C. By comparison, the frequency distributions of the reference group (Cases 8, 10, 12, and 13) turned out to be widespread gentle curves with peak values markedly away from 22.0°C. The results of the reference group show that these locations do not represent the occupancy zone's temperature well. Furthermore, between the occupancy-zone-focused Cases 9 and 13 and the entire-space-equally-weighted Cases 7 and 11, in Pattern 1, Case 9's frequency at 22.0°C is larger than Case 7's. In Pattern 2, although this trend is not as clear, the standard deviation is improved in Case 13 in the occupancy zone level, which can be observed from Table 6. The validity of this method can be verified and so can the effectiveness of the weighting factors.

6. Conclusions

1. Methods for room temperature fluctuation analysis and optimization of air-conditioner sensor location are proposed. The validity of the proposed method is confirmed through a case study.

2. By visualizing the contribution ratio of each heat source in the form of CRI, the influence of the sensor location and the characteristics of room temperature fluctuation can be analyzed.

3. The authors proposed a scalar objective function that reflects the temperature fluctuation characteristics and enables the quantitative evaluation of different sensor location.

4. In the case study, a sensor location minimizing the room temperature fluctuation was found.

Notes

[1] The flow field is fixed to simplify the heat transport phenomenon. In other words, the heat flow to be transported in the designed flow field controlled by the air conditioning system is analyzed.

[2] This work was conducted when the first author belonged to the listed university.

References

1) Uno, T., *et al.* (2012) Reduction of Energy Consumption by AC due to Air Tightness and Ventilation Strategy in Residences in Hot and Humid Climates, Journal of Asian Architecture and Building Engineering, Vol. 11, pp.407-414.
2) American Society of Heating, Refrigerating and Air-Conditioning Engineers. (2007) 2007 ASHRAE Handbook - HVAC Applications. SI ed. America: American Society of Heating.
3) Nevins, R.G. and Ward E. D. (1968) Room Air Distribution with an Air Distributing Ceiling. ASHRAE Transactions, Vol. 74, Part 1.
4) Kato, S., Kobayashi, H. and Murakami S. (1998). Scales for Assessing Contribution of Heat Sources and Sinks to Temperature Distributions in Room by Means of Numerical Simulation. Transactions of the Society of Heating, Air-Conditioning and Sanitary Engineers of Japan. Vol. 69, pp.39-47.
5) Sempey, A., Inard, C., Ghiaus, C. and Allery, C. (2009). Fast simulation of temperature distribution in air conditioned rooms by using proper orthogonal decomposition, Building and Environment, Vol. 44, Issue 2, pp.280-289.
6) Harayama, K., Honda, M. and Kaseda, C. (2009). Ichijōhō to Bunpukei shimyurēshon wo riyōshita hitoshūhen no kyokusho onnetsu kankyō seigyo gijutsu no kaihatsu, Summaries of technical papers of Annual Meeting, Architectural Institute of Japan, 80(II), pp.1-4. (in Japanese)
7) Harayama, K., Honda, M. and Kaseda, C. (2010). CFD kaiseki wo mochiita kyokusho onnetsu kankyō seigyo gijutsu no kaihatsu, Summaries of technical papers of Annual Meeting Architectural Institute of Japan., pp.1161-1162. (in Japanese)
8) Harayama, K., Saisu, Y., *et al.* (2011). Establishment of a Validation Environment for Local Air-conditioning Control Technology (Part 1) Development of 'ambican' Combined Air-Conditioning Unit Simulator with CFD Analysis. Architectural Institute of Japan, pp.1353-1354.
9) Murata, H., Harayama, K., *et al.* (2011). Establishment of a Validation Environment for Local Air-conditioning Control Technology (Part 2) Study of Energy Saving and Thermal Comfort on Local Thermal Comfort Control Technology. Architectural Institute of Japan, pp.1355-1356.
10) Ueda, T. and Honda, N. (2008). A Study on Gain-Scheduled HVAC Control Based on Fuzzy Models in Large Spaces, Transactions of the Society of Heating, Air-Conditioning and Sanitary Engineers of Japan (134), pp.31-38.
11) Abe, k. Momose, K. and Kimoto, H. (2004) Optimization of Natural Convection Field Using Adjoint Numerical Analysis, The Japan Society of Mechanical Engineers (B) Vol. 70, No. 691, pp.167-174.
12) Hiyama, K. and Kato, S. (2011) Optimization of variables in air-conditioning control systems: Applications of simulations integrating CFD analysis and response factor method, Building Simulation, Vol. 4, No. 4, pp.335-340.
13) Hiyama K, Kato S. (2011) Integration of three-dimensional CFD results into energy simulations utilizing an advection-diffusion response factor, Energy and Buildings, Vol. 43, pp.2752-2759.
14) Zhang, W., Kato, S. and Ishida, Y. (2010) Calculation Method of Contribution Ratio of Indoor Climate (CRI) by Means of Setting a Uniform Heat Sink in Natural Convection Air Flow Field, Journal of Environmental Engineering 75(658), pp.1033-1040.
15) Zhang, W., Hiyama, K., Kato, S. and Ishida, Y. (2013) Building energy simulation considering spatial temperature distribution for nonuniform indoor environment, Building and Environment, Vol. 63, pp.89-96.
16) Institute for Building Environment and Energy Conservation (IBEC). (2010) Jūtakujigyōkenchikushu no handankijun no gaiyō, pp.7-13, Ver 1.1. Tokyo: IBEC. (in Japanese)